energies

MDPI

Article

Effects of Diesel Injection Timing on Combustion and Emission Characteristics of a Dual-Fuel Engine Fueled with Isopropanol–Butanol–Ethanol (IBE) and Pilot Diesel

Xiao Liu [1], Kaijie Li [1], Yanxin Zhao [1], Gang Li [1,*] and Jinhai Wang [2]

[1] College of Mechanical and Electronic Engineering, Northwest A&F University, Yangling 712100, China; liuxiao1179748025@163.com (X.L.); jerrym555@163.com (K.L.); a17513270323@163.com (Y.Z.)
[2] School of Mechanical Engineering, Beijing Institute of Technology, Beijing 100081, China; wjh20230516@163.com
* Correspondence: cn_ligang@163.com or cn_ligang@nwafu.edu.cn

Abstract

The dual-fuel combustion strategy is a promising method to achieve the high-ratio utilization of isopropanol–butanol–ethanol (IBE) in diesel engines. However, how the diesel injection timing affects the combustion and emission characteristics of the diesel/IBE dual-fuel engine has been seldom systematically studied. In this regard, experiments were conducted on a diesel/IBE dual-fuel engine with the engine load fixed at 50% and the engine speed fixed at 1600 rpm, while the co-combustion ratio of IBE to diesel varied from 20.51% to 52.56%. The results show that both the peak in-cylinder pressure and maximum heat release rate increase as the diesel injection timing advances, resulting in the brake thermal efficiency of the diesel/IBE dual-fuel engine increasing. For emissions, CO emissions always decrease as the diesel injection timing advances, while HC emissions increase with the diesel injection timing either delayed or advanced. Furthermore, although the NO_2 emissions first increase and then decrease as the diesel injection timing advances, the NO emissions continue to increase, leading to an overall increase in NO_x emissions. However, whether the diesel injection timing is advanced or delayed, PN emissions are significantly reduced. That is to say, delaying the diesel injection timing can simultaneously reduce NO_x and PN emissions in a diesel/IBE dual-fuel engine.

Keywords: isopropanol–butanol–ethanol (IBE); diesel/IBE dual fuel; combustion; performance; emissions

Check for updates

Academic Editor: Maria Founti

Received: 23 July 2026
Revised: 25 August 2026
Accepted: 26 August 2026
Published: 29 August 2026

Copyright: © 2026 by the authors. Licensee MDPI, Basel, Switzerland. This article is an open access article distributed under the terms and conditions of the Creative Commons Attribution (CC BY) license.

1. Introduction

Diesel engines are vital power sources in vehicles, ships, agricultural equipment, and other fields, owing to their high engine torque and adaptability to diverse applications [1,2]. However, NO_x and soot emissions produced by diesel engines are at a high level, which is detrimental to the environment and human health [3,4]. Meanwhile, emission regulations for engines are becoming increasingly stringent worldwide, meaning diesel engines have to adopt new energy-saving and emission-reduction technologies to address these challenges [5]. In many studies, the dual-fuel combustion strategy exhibits great potential for reducing traditional fossil fuel consumption and soot emissions [6,7]. At present, this method has received widespread attention from scholars, and related research has been conducted [8].

Among the various additives, alcohol has attracted the most research attention from scholars [9,10], thanks to its superior combustion performance, low pollution, abundant sources, and low cost [11]. Bhumula et al. [12] studied 1-heptanol/diesel fuel mixtures. They concluded that it could limit NO_x as well as soot emissions. In high SOI (Start of Injection) and large load conditions, the BTE increased by 6.21% compared with the standard SOI. Chockalingam et al. [13], using methanol, propanol, and diesel fuel in different proportions to obtain four mixtures of fuel blends to test these blends, found that NO_x emissions were significantly reduced, and the fuel mixtures not only had good combustion characteristics but also low pollution. Therefore, most scholars have studied these fuel mixtures. It was found that increasing the propanol content significantly reduced NO_x emissions but increased HC emissions. Killol et al. [14] blended n-butanol with Karanja methyl ester and studied the characteristics of the mixture. They found that NO_x emissions decreased in most cases, and BTE generally increased. When the engine load increased, both HC and CO emissions decreased. Yilmaz et al. [15] conducted experiments using 1-butanol/biodiesel blends and regular diesel fuel. By comparing the emission characteristics, they found that 1-butanol/biodiesel blends not only significantly decreased NO_x emissions but also reduced the polycyclic aromatic hydrocarbon (PAH) emissions (carcinogenic pollutants). But, due to the addition of 1-butanol, HC and CO emissions increased. These studies suggest that butanol has better performance when blended with diesel fuel. Compared to other lower alcohols, butanol exhibits superior miscibility, higher energy density, and a higher cetane number. Also, butanol is a better choice for blending, as it has lower evaporation pressure and a lower auto ignition point [16]. When butanol is produced through fermentation, a mixture consisting of acetone, n-butanol, and ethanol (ABE) is generated. The ratio of various alcohols in this mixture is approximately 3:6:1 [17]. Then, the mixture needs to be separated to obtain pure butanol. However, the separation cost is relatively high, and the efficiency is not satisfactory [18,19]. Therefore, some scholars have blended ABE directly with fuel and then tested the engine performance when burning the mixture. For example, Xu et al. [20] blended ABE with diesel fuel and then studied the evaporation phenomenon. They introduced the evaporation stages of blended droplets, which helps scholars gain insight into the combustion mechanism. Çakmak [21] blended ABE and butanol with diesel and compared two blended fuels. Their research indicated that all the blended fuels decreased NO and soot emissions, while ABE had a lower cost of production. Therefore, they hold the view that ABE has better application prospects. Veza et al. [22] studied the impact of ABE–diesel blends on homogeneous charge compression ignition (HCCI) engines. The results show that the blended fuels have lower CO_2 and NO_x emissions, indicating improved combustion efficiency. Although ABE-diesel blends have numerous advantages, acetone, one component of ABE, is corrosive to rubber and may reduce engine life. In addition, acetone's low flash point makes it dangerous during transport [23]. Therefore, a further fermentation technique was utilized to convert acetone into isopropanol. The new mixture obtained through this method is isopropanol–butanol–ethanol (IBE). The flash point of acetone is about 253 K, while the flash point of isopropanol is approximately 284.5 K. Isopropanol has a higher flash point and lower corrosivity. Overall, IBE is not only relatively safe but also has a higher energy content compared to ABE. Therefore, it has garnered widespread attention in recent years. Lee et al. [24] tested the IBE/diesel blend in a single-cylinder diesel engine. The study found that soot emissions decreased, while NO_x emissions increased. Meng et al. [25] combusted IBE/diesel blends with different mixing ratios using the spark-assisted compression ignition (SACI) technique and concluded that increasing the energy ratio of ethanol and isopropanol was beneficial in reducing $BSNO_x$ and BSHC emissions.

Notably, the above approach improves engine performance by blending the fuel with diesel in a specific ratio prior to combustion. However, this method utilizes alcohol fuel inefficiently and fails to take full advantage of its benefits. Therefore, scholars have studied the further application of alcohol fuel through the dual-fuel combustion strategy. The implementation of this strategy involves direct injection and port injection [26]. Through these two methods, the CCR of alcohol fuel can be significantly improved. In addition, this strategy also helps to enhance the combustion and emission characteristics of the diesel engine. Meanwhile, Dempsey et al. [27] studied the influence of multiple diesel injections under reactivity-controlled compression ignition (RCCI) mode. Through this experiment, they found that when the methanol substitution rate was 66.5%, the engine exhibited high thermal efficiency and low emissions, but fuel consumption increased. Wei et al. [28] conducted experiments on a 6-cylinder turbocharged diesel engine and indicated that under low-load conditions, the premixed ratio of methanol (PR_m) can reach up to 70%, and the PR_m can still exceed 40% under high-load conditions. Additionally, their research showed that dry soot emissions can be effectively reduced at high PR_m, and the trade-off relationship between NO_x and dry soot emissions is disrupted. This further demonstrates that the dual-fuel combustion strategy can effectively increase alcohol fuel utilization and significantly reduce soot emissions. Splitter et al. [29] conducted research on a 145 mm-bore single-cylinder engine, and their findings indicated that the maximum methanol fuel equivalence ratio (MFE) can reach 75%. Park et al. [30] used numerical simulation to study the combined combustion strategy with methanol port injection. The results showed that the introduction of methanol significantly reduced the in-cylinder temperature, in-cylinder pressure, and NO_x emissions, while fuel consumption increased. In addition, Geng et al. [31] studied the particulate matter (PM) emissions from diesel/methanol dual-fuel engines. In their research, the methanol substitution rate reached 40%, significantly reducing particulate matter emissions. Agudelo et al. [32] investigated the effects of n-butanol and hydrous ethanol on a dual-fuel engine. The results showed that both alcohols reduced NO_x and PM emissions, but THC and CO emissions increased. In addition, Wu et al. [33] conducted experiments on a single-cylinder diesel engine. The maximum ethanol premix ratio was 30%. Their research also confirmed that the emissions of the engine were effectively reduced.

The aforementioned studies have proven that the addition of IBE into diesel is capable of reducing fossil fuel consumption and soot emissions in diesel engines [34]. However, the blending ratio of IBE to diesel is limited since blending IBE to diesel may deteriorate the ignitability of diesel. The dual-fuel combustion strategy is a promising method to achieve the high-ratio combustion of alcohol fuels in diesel engines, but there are few studies focusing on the combustion, performance and emissions of the diesel/IBE dual-fuel engine. And how the diesel injection timing (DIT) affects the combustion process and emission formation of diesel/IBE dual-fuel engines has been scarcely studied to date. In this regard, in this research a diesel engine was modified into a diesel/IBE dual-fuel engine to study how the DIT affects its combustion, performance and emissions. Especially, NO, NO_2 and particulate emissions were studied to find a method to reduce them simultaneously.

2. Materials and Methods

2.1. Engine and Test Equipment

The original diesel engine (Guangxi Yuchai Machinery Group Co., Ltd., Guangxi, China) is a four-cylinder electronically controlled high-pressure common rail diesel engine. More detailed information about the diesel engine is shown in Table 1, and a diagram of the engine test bed is shown in Figure 1. Some modifications were made to the engine to enable it to operate in diesel/IBE dual-fuel combustion mode. The main modification to

the original diesel engine involved installing a fuel supply system capable of achieving IBE supply and injection. The system primarily consists of an IBE fuel tank, a dedicated pump, a fuel filter, a fuel-pressure-regulating valve, and two injectors. Specifically, the two fuel injectors were deployed for port fuel injection (PFI), with each unit mounted on the intake pipe. In addition, there was also a customized electronic control unit (ECU). This ECU was used to control the injection parameters of the IBE. During the experiment, the pump extracted IBE from the tank, filtered it through a filter, and delivered it to the two injectors installed on the intake port. Then, IBE was injected into the intake pipe. In this way, IBE was mixed with air to form a homogeneous gas mixture. The mixture entered the cylinder and was ignited by the direct-injected pilot diesel. During this process, the fuel-pressure-regulating valve maintained the pressure of IBE at 0.3 MPa. Both the IBE injection timing and pulse width were precisely adjusted by the IBE ECU. And the original engine's ECU was used to adjust diesel injection parameters. The original engine's ECU and IBE ECU were independent of each other but shared the same signals, such as crank angle signals, coolant temperature signals and so on.

Table 1. Specifications of the diesel engine.

Items	Specifications
Type	Vertical, in-line, four-stroke, direct injection
Inspiratory mode	Turbocharged intercooled
Fuel injection system	Electronically controlled common-rail
Bore × stroke	102 mm × 118 mm
Displacement	3.857 L
Compression ratio	17.5:1
Intake valve opening	14 °CA before top dead center
Intake valve closing	38 °CA after bottom dead center
Exhaust valve opening	54 °CA before bottom dead center
Exhaust valve closing	14 °CA after top dead center
Rated power	95 kW (3000 rpm)
Maximum torque	380 N m (1600–2240 rpm)

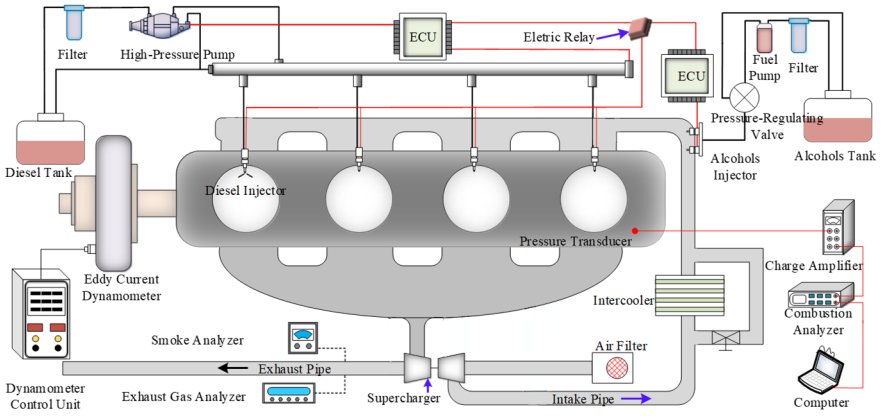

Figure 1. Schematic of experimental apparatus.

The test bed mainly includes the original diesel engine, an exhaust gas analyzer, a combustion analyzer, a dynamometer, a pressure sensor, an oxygen sensor, an IBE injection system and an electronic control system. The dynamometer and the engine control system serve as the core equipment for engine control. The dynamometer model is CW160 (Xiangyi Dynamometer Co., Ltd., Changsha, China), while the control system model is FC2000 (Xiangyi Dynamometer Co., Ltd., Changsha, China). These two devices are jointly responsible for controlling the torque and speed of the engine during the experiment. For

the IBE and diesel consumption, they were measured by two high-precision electronic balances (model EX-E650, Shenzhen Anheng Weighing Instrument Electronics Co., Ltd., Shenzhen, China), and the CCR and EQBSFC were calculated based on these data. The measurement ranges of the two balances are 0–5 kg and 0–30 kg, respectively. For emissions, an exhaust gas analyzer was used to measure exhaust emissions. This advanced analyzer (model MET 6.3, MAHA Maschinenbau (Beijing) Trading Co., Ltd., Beijing, China) can detect various emissions, such as CO, HC and NO_x emissions. Notably, both standard gas and zero gas were used to calibrate the analyzer before the experiment to ensure accuracy. Additionally, this study used a particle-counting instrument (model DiTEST Counter Mobile, MAHA Maschinenbau (Beijing) Trading Co., Ltd., Beijing, China) to measure PN. This particle counter was produced by MAHA company. The DiTEST Counter Mobile utilizes the Advanced Diffusion Charging principle. It uses corona discharge to impart a unipolar charge to particulates in the exhaust gas, which are then collected in the Faraday cage through pulse electrostatic precipitation. The current signal is processed and converted into particulate matter concentration. The calculation method is based on Equation (1). During this study, a diluter at a ratio of 5:1 was used, ensuring that the measured value fell within the range of the instrument.

$$PN = \frac{I}{q \times Q} \times K \quad (1)$$

where I is the current (A); q is the average charge of each particle (C); Q is the flow rate sampled from the exhaust pipe (cm^3/s); and K is a correction factor.

The pressure transducer (6052C, Kistler, Kistler Group, Winterthur, Switzerland) used in this study has high accuracy and exhibits reliable temperature resistance. Based on the piezoelectric effect, this transducer is capable of converting pressure signals into electrical signals. And the transducer was installed at the corresponding position on the cylinder head of the first cylinder. During the experiment, the electrical signal output from the transducer was processed by a charge amplifier (5019, Kistler, Kistler Group, Winterthur, Switzerland). Then, a combustion analyzer recorded the signal. Moreover, the corresponding crank angle was obtained through a crank angle encoder. For each operating condition, the combustion analyzer recorded three sets of in-cylinder pressure data, with each set containing 150 cycles. The sampling interval of the combustion analyzer was 0.1 °CA (Crank Angle). The average in-cylinder pressure curve was calculated from a total of 450 cycles. Then, the HRR and CD were derived from the in-cylinder pressure. During the study, all data were recorded three times in a stable state to ensure accuracy and reproducibility and to reduce uncertainty. The accuracy of all instruments is shown in Table 2. There is more detailed information about the experimental setup and test systems in Ref. [35].

Table 2. Accuracy of measured parameters.

Measured Parameters	Equipment	Range	Accuracy	Uncertainty (%)
Engine torque	CW160	0–600 N m	±0.2%FS	0.2
Engine speed		0–8000 rpm	±1 rpm	0.0125
Cylinder pressure	Kistler 6052C	0–25 MPa	±0.5%	0.5
IBE mass	EX-E650	0–5 kg	±0.1 g	0.002
Diesel mass	EX-E650	0–30 kg	±0.1 g	0.00033
Soot emission	AVL DiTEST	1000–5,000,000 $1/cm^3$	1000 $1/cm^3$	2.03
CO emission	MET6.3	0–15%	±0.001%	0.72
HC emission		0–10,000 ppm	±1 ppm	0.12
NO_2 emission		0–500 ppm	±1 ppm	0.32
NO emission		0–1000 ppm	±1 ppm	0.18

2.2. Fuel Introduction and Preparation

The diesel used in the experiment was ultra-low-sulfur commercial diesel meeting China VI specification, with a sulfur content of less than 10 ppm. The isopropanol, n-butanol, and ethanol used for preparing the IBE were of analytical grade purity. To simulate the typical component distribution in IBE fermentation production as realistically as possible, the volume ratio of different IBE components used in the study was 3:6:1. The components corresponding to this ratio were isopropanol, n-butanol and ethanol. The three components were fully stirred using a blender until the IBE mixture was ready for testing. Then, the IBE was allowed to stand for two weeks to ensure that no stratification occurred. Table 3 shows some physicochemical properties of fuels used in this study. Notably, the properties of test fuels were sourced from Ref. [36]. As for the IBE mixture, the detailed physicochemical properties were determined through the method in Ref. [36].

Table 3. Physicochemical properties of test fuels.

Parameters	Diesel	Ethanol	Isopropanol	n-Butanol	IBE
Chemical formula	C_{10}–C_{22}	C_2H_5OH	C_3H_7OH	C_4H_9OH	-
Octane number	20–30	108	112	96	103
Cetane number	40–55	5–8	12	17	13.9
Viscosity (cSt)	2–3.5	1.2	2.4	2.98	2.28
Oxygen content (wt.%)	0	34.7	26.6	21.6	24.4
Boiling temperature (K)	450–643	351	357	391	-
Density (kg/m^3)	820–850	795	786	813	803
Stoichiometric AFR	14.3	9.0	10.4	11.21	10.7
Latent heat (kJ/kg)	250–290	900	758	707	711
Lower heating value (MJ/kg)	42.5	26.8	30.4	33.1	31.7
Saturated vapor pressure (kPa)	0.3	13.8	6.7	2.27	5.56
Auto-ignition temperature (K)	503	707	672	658	-

2.3. Experimental Procedure

This study aims to find out how the DIT affects the diesel/IBE dual-fuel engine. However, numerous studies have shown that excessively high or low loads can affect the CCR. Therefore, the engine load in this experiment was consistently maintained at 50%, with a corresponding engine speed of 1600 rpm. Under this operating condition, the DIT of the original diesel engine was approximately 7 °CA BTDC. During the experiment, this DIT was used as the baseline. There were five DIT values (5, 6, 7, 8, 9 °CA BTDC) chosen under three CCR conditions of 20.51%, 37.06% and 52.56% in this investigation. In order to more intuitively display the usage ratio of IBE corresponding to each CCR, this study used the percentage of the mass (wt.%) to represent the IBE substitute ratio (%). In addition, before the start of the test, the ambient temperature was 12 °C and the ambient pressure was 0.092 MPa, while the boost pressure during the experiment was maintained at 0.1 MPa. To start with, the engine ran at idle speed in original mode until the engine oil temperature rose to 95 °C and water temperature rose to 80 °C. After that, the study was started. The engine was then adjusted for IBE injection pulse width, and the diesel injection pulse width was adjusted to stabilize the engine condition at 50%. During the test, the IBE injection pulse width was adjusted first, followed by the adjustment of the injection timing. The diesel fuel injection was then adjusted to stabilize the engine at 50% load. Once stable, three sets of data were recorded under each experimental condition. The aim of recording data repeatedly is to enhance accuracy and reliability. Table 4 is the operating conditions of this study.

Table 4. Test conditions.

Items	Case 1	Case 2	Case 3
Engine load (%)		50	
Engine speed (rpm)		1600	
Engine torque (N m)		190	
Diesel injection pressure (MPa)		90	
IBE injection pressure (MPa)		0.3	
Diesel mass flow (kg/h)	5.52	4.51	3.53
IBE mass flow (kg/h)	1.91	3.56	5.24
CCR (%)	20.51	37.06	52.56
Substitution ratio (%)	25.71	44.11	59.77
Diesel injection timing (°CA BTDC)		5, 6, 7, 8, 9	

2.4. Data Analysis

2.4.1. Combustion Phasing

Ignition delay (ID) and combustion duration (CD) are important indicators for evaluating the combustion of an engine. In this study, the start and end of combustion were defined as SOC and EOC. Both the SOC and EOC were defined based on the total heat. When 10% of the total heat is released, the SOC is determined. Similarly, the EOC is defined as the point when 90% of the total heat is released. The detailed content can be seen in Figure 2. Moreover, the method to calculate the net heat release rate is as follows:

$$\frac{dQ}{d\theta} = \frac{\gamma}{\gamma - 1} P \frac{dV}{d\theta} + \frac{1}{\gamma - 1} V \frac{dP}{d\theta} \tag{2}$$

where γ is the ratio of specific heats, with a value of 1.37, P is the in-cylinder pressure and V is the volume. Based on these data, ID is the crank angle from the DIT to the SOC, while CD is the crank angle from the SOC to the EOC.

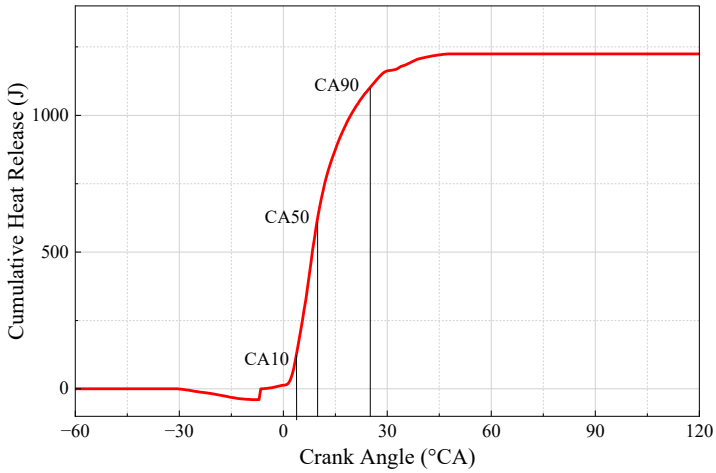

Figure 2. The crank angle corresponding to CA10, CA50, and CA90 obtained from CHR.

2.4.2. The Brake Thermal Efficiency

To visually display and compare the dual-fuel engine performance, the BTE was a standard parameter. The calculation formula is as follows:

$$BTE = 3.6 \times \frac{P_e}{\dot{m}_I \times LHV_I + \dot{m}_d \times LHV_d} \tag{3}$$

where P_e is the engine power (kW) and $\dot{m}_I$ and $\dot{m}_d$ are the mass flow rate of IBE and diesel (kg/h). LHV_I and LHV_d are the low heating value of IBE and diesel (MJ/kg), respectively.

2.4.3. The Brake Specific Fuel Consumption

It is unreasonable to directly judge engine performance based on fuel consumption due to the lower heating value of IBE and diesel being different. Therefore, this study adopted equivalent BSFC (EQBSFC), which can evaluate the fuel economy of the dual-fuel engine more accurately. The formula used in this study is as follows:

$$EQBSFC = \frac{(\dot{m}_I \times LHV_I + \dot{m}_d \times LHV_d)}{P_e \times LHV_d} \times 1000 \quad (4)$$

In the equation, the meanings of P_e, LHV_I and LHV_d are the same as in Equation (3).

2.4.4. IBE Co-Combustion Ratio

The diesel/IBE dual-fuel engine used IBE and diesel. These two fuels were low and high reactivity fuel, respectively. Compared to the volume ratio, the energy ratio can better reflect the effect of IBE. Therefore, the energy provided by IBE needs to be calculated. The co-combustion ratio (CCR) is used in this study to reflect this ratio. The CCR calculation method used in this study is as follows:

$$CCR = \frac{\dot{m}_I \times LHV_I}{\dot{m}_I \times LHV_I + \dot{m}_d \times LHV_d} \times 100\% \quad (5)$$

In the equation, the meanings of $\dot{m}_I$, LHV_I and LHV_d are the same as in Equation (3).

2.4.5. Emissions

Due to differences in engine displacement, power, and test conditions, it is inappropriate to directly compare the emissions. Therefore, it is necessary to normalize the emissions. For example, HC emissions are converted to BSHC (g/kW·h). The CO, NO, and NO_2 also need to be normalized. The equations used for conversion are as follows:

$$BSHC = HC \times \frac{\left(\dot{m}_{air} + \dot{m}_{fuel}\right) \times 0.479}{1000 \times P_e} \quad (6)$$

$$BSCO = CO \times \frac{\left(\dot{m}_{air} + \dot{m}_{fuel}\right) \times 0.966 \times 1000}{100 \times P_e} \quad (7)$$

$$BSNO_x = NO_x \times \frac{\left(\dot{m}_{air} + \dot{m}_{fuel}\right) \times 1.587}{1000 \times P_e} \quad (8)$$

$$BSNO = NO \times \frac{\left(\dot{m}_{air} + \dot{m}_{fuel}\right) \times 1.34}{1000 \times P_e} \quad (9)$$

$$BSNO_2 = NO_2 \times \frac{\left(\dot{m}_{air} + \dot{m}_{fuel}\right) \times 2.05}{1000 \times P_e} \quad (10)$$

$$\dot{m}_{fuel} = \dot{m}_d + \dot{m}_I \frac{LHV_I}{LHV_d} \quad (11)$$

where $\dot{m}_{air}$ and $\dot{m}_{fuel}$ are the mass flow rate of air and fuel (kg/h).

3. Results

3.1. Impact on Combustion

3.1.1. Combustion Characteristics

Figure 3 shows the in-cylinder pressure and HRR for different CCRs at various DITs. It is obvious that the P_{max} increases with the advance of DIT. When the DIT advances from 5 °CA BTDC to 9 °CA BTDC, the P_{max} increases by 16.1%, 17.8%, and 17.1% for the CCRs of 20.51%, 37.06%, and 52.56%. The reason for this result is that IBE can effectively reduce the in-cylinder temperature. The earlier DITs provide better in-cylinder thermal conditions for diesel injection, which improves fuel atomization. In addition, due to the shorter mixing time, the resulting mixture has a higher degree of stratification, which also helps to form a fuel enrichment zone and facilitates the spontaneous combustion of atomized fuel. Meanwhile, the crank angle corresponding to the P_{max} also advances. This indicates that advancing the DIT significantly affects the combustion of the dual-fuel engine. Notably, as the DIT advances, the P_{max} exhibits a relatively uniform linear change when the CCR is 20.51% and 52.56%. This aligns with the findings of Enzhe Song et al. [37], who conducted numerical simulations and concluded that under varying loads, advancing the DIT by 1 °CA can result in a P_{max} increase of approximately 0.2–0.3 MPa. When the DIT is the same, the P_{max} is higher under the higher CCR, which is consistent with previous research.

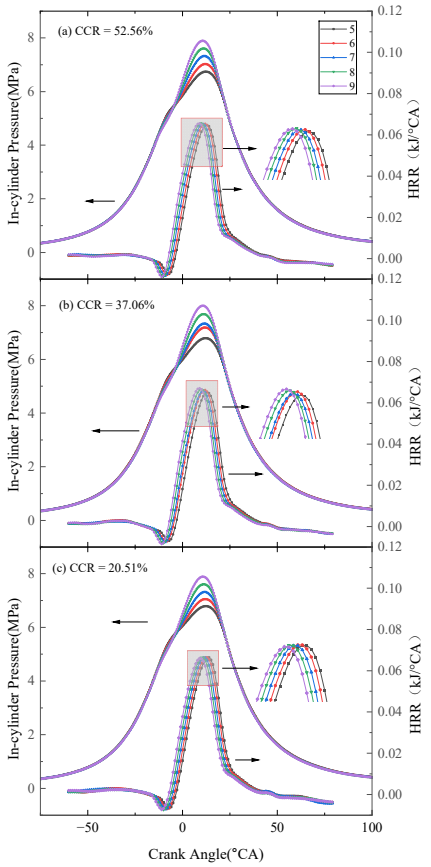

Figure 3. In-cylinder pressure and HRR with various diesel injection timing.

In addition, it also shows that as the DIT advances, the overall HRR curves show a significant advance under different CCRs. This is because IBE cannot auto-ignite under compression, and thus DIT exerts a significant influence on the ignition timing of combustion. As the DIT advances, the ignition timing of IBE also advances. At the same time, at CCRs of 20.51% and 37.06%, the maximum HRR increases with the advance of DIT. This is because the diesel fuel has a longer mixing period inside the cylinder, enabling more

sufficient combustion of IBE. However, when the CCR is 52.56%, it actually decreased. This may be due to the excessively high CCR, which leads to a lower in-cylinder temperature, unfavorable in-cylinder conditions during diesel injection, and weakened stratification of the mixture, thus deteriorating the combustion process [38].

3.1.2. Impact on Ignition Delay and Combustion Duration

Figure 4 shows the effect of DIT on ID and CD. When the CCR is 20.51% and 37.06%, the ID prolongs as the DIT advances. By contrast, the ID remains nearly constant at a CCR of 52.56%. The CD also extends when the DIT advances. The reason affecting the ID and CD can be analyzed as follows. First, IBE has a high latent heat of vaporization. This indicates that IBE can effectively reduce the cylinder temperature, thereby prolonging the ID and CD. Meanwhile, an earlier DIT also prolongs the ID, and their coupled effect further prolongs the ID. At a high CCR, the cooling effect induced by IBE is further enhanced. In this case, advancing the DIT provides a more favorable thermal atmosphere for the injected fuel and promotes fuel atomization. Consequently, further advancement of the DIT no longer leads to an increase in ID. Moreover, at a fixed DIT, the higher the CCR, the shorter the ID. This is mainly because the oxygenated property of IBE can effectively improve the oxygen-deficient condition in the cylinder. This is beneficial to the combustion of fuel, thereby shortening the ID. However, the CD extends with the increase in the CCR. This phenomenon is probably attributed to the high proportion of IBE in the mixture, which reduces the chemical reactivity of the fuel–air mixture and ultimately prolongs the CD.

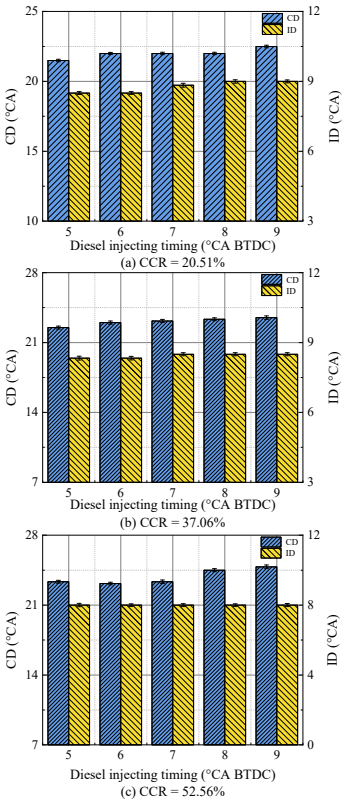

Figure 4. ID and CD with various diesel injection timing.

3.2. Engine Performance

Figure 5 shows the variation in BTE and EQBSFC of the engine for different DIT conditions in this study. It is obvious that when the DIT is the same, the BTE decreases notably with the increase in the CCR. This is attributed to the fact that a higher IBE proportion can significantly reduce the in-cylinder temperature. This not only results in an

excessive drop of in-cylinder temperature, which is unfavorable for diesel atomization, but also leads to energy loss.

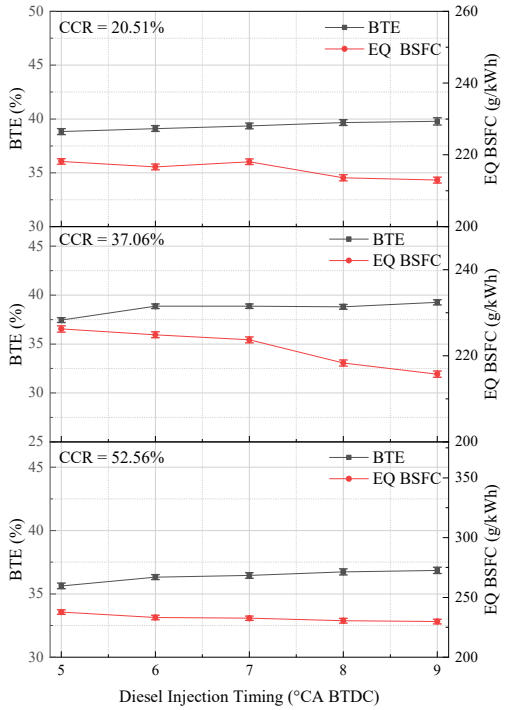

Figure 5. BTE and EQBSFC with various diesel injection timing.

When the CCR remains constant, BTE increases as the DIT advances. Furthermore, this increase can be divided into two stages. Initially, when the DIT advances from 5 °CA BTDC to 8 °CA BTDC, the BTE for medium and low CCRs experiences a significant increase, but the change becomes less pronounced as the DIT continues to advance. This is attributed to the large heat of vaporization of IBE, which leads to greater energy loss. However, earlier DIT facilitates earlier combustion of IBE, reducing the cooling duration. Consequently, energy loss decreases, and BTE increases significantly. Subsequently, as the DIT becomes too advanced, combustion occurs further from TDC, which affects the combustion process and thereby slows down the trend of BTE increase. For BTE at a high CCR, there is a notable increase when the DIT advances from 5 °CA BTDC to 6 °CA BTDC, but the subsequent increase becomes more gradual. This is because at a higher CCR, the cooling effect of IBE is stronger, diminishing the effectiveness of optimizing DIT, thus resulting in a less pronounced increase. In addition, due to the advance of DIT, the degree of mixing between diesel and IBE is increased, leading to more complete combustion. Therefore, there is a decrease in EQBSFC. Meanwhile, it is evident that a higher CCR corresponds to a lower BTE and higher EQBSFC. It can be explained that the higher CCR exacerbates local misfiring and incomplete combustion. Furthermore, the higher CCR increases the IBE entering the cylinder, leading to increased heat loss. Therefore, to maintain the engine load and increase fuel demand, the EQBSFC also increases accordingly.

3.3. Emission Characteristics

3.3.1. CO and HC Emissions

Figure 6 shows the levels of CO and HC emissions in three CCRs for different DITs. Obviously, when the CCR is 37.06% and 52.56%, CO emissions decrease as DIT advances, but the subsequent change is little. However, when the CCR is 20.51% and DIT advances excessively, CO emissions actually increase. The reason for the decrease may be that as DIT advances, the in-cylinder temperature rises, reducing CO emissions. In addition, the

time for IBE to enter the cylinder is relatively short, so the formed mixture is not too lean. The concentration of IBE in these areas is higher, and more oxygen-containing radicals are generated, which leads to better oxidation of CO during combustion. When the CCR is 20.51%, on one hand, due to the low content of IBE and limited oxygen-containing radicals, CO cannot be fully oxidized, which results in a limited reduction in CO emissions. Furthermore, as the DIT advances, the lower IBE proportion can lead to an excessively lean air–fuel mixture, which induces incomplete combustion and a rise in CO emissions. HC emissions exhibit a trend of first decreasing and then increasing as the DIT advances at all CCRs. This is due to the fact that advancing the DIT initially can increase the temperature, reducing HC emissions. However, when the DIT is excessively advanced, the IBE in regions with high concentration cannot be fully burned, resulting in an increase in HC emissions. Additionally, earlier DIT may lead to trapped fuel in crevices that cannot be burned, thus also contributing to an increase in HC emissions. Similar to CO emissions, the higher CCR causes higher HC emissions when the DIT is the same. This also indicates that a higher CCR can lead to incomplete combustion of fuel, which is detrimental to energy conservation and emission reduction in diesel engines.

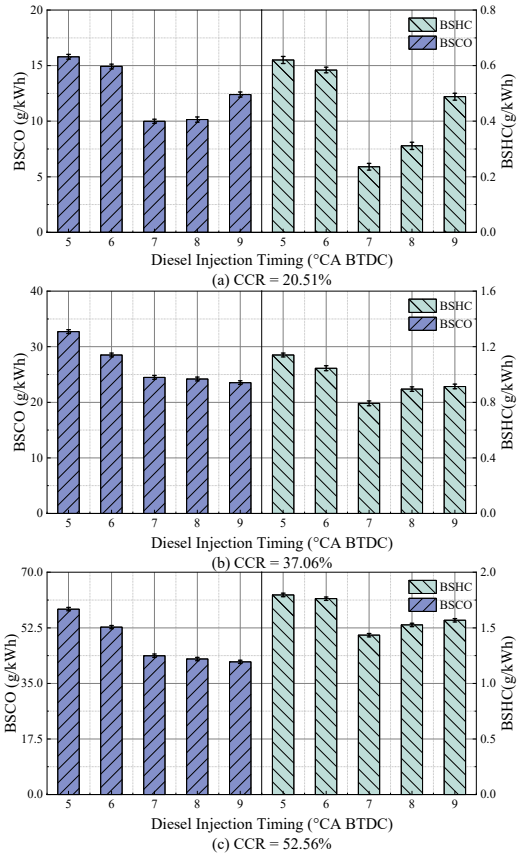

Figure 6. CO and HC emissions with various diesel injection timing.

3.3.2. NO and NO_2 Emissions

Figure 7 shows NO and NO_2 emissions in the exhaust gas under various DITs. On the whole, when the DIT is the same, BSNO and $BSNO_2$ decrease with the increase in CCRs. For NO emissions, it mainly follows the Zeldovich mechanism, which relies on high in-cylinder temperature. With the increase in CCRs, the IBE proportion increases. The cooling effect of IBE is more significant, causing a greater decrease in in-cylinder temperature. This makes the in-cylinder environment not conducive to the formation of NO_x, leading to a decrease in NO emissions. The main source of NO_2 is the oxidation of NO, and the lower in-cylinder

temperature is also not conducive to the further conversion of NO to NO_2, so NO_2 also has a certain decline.

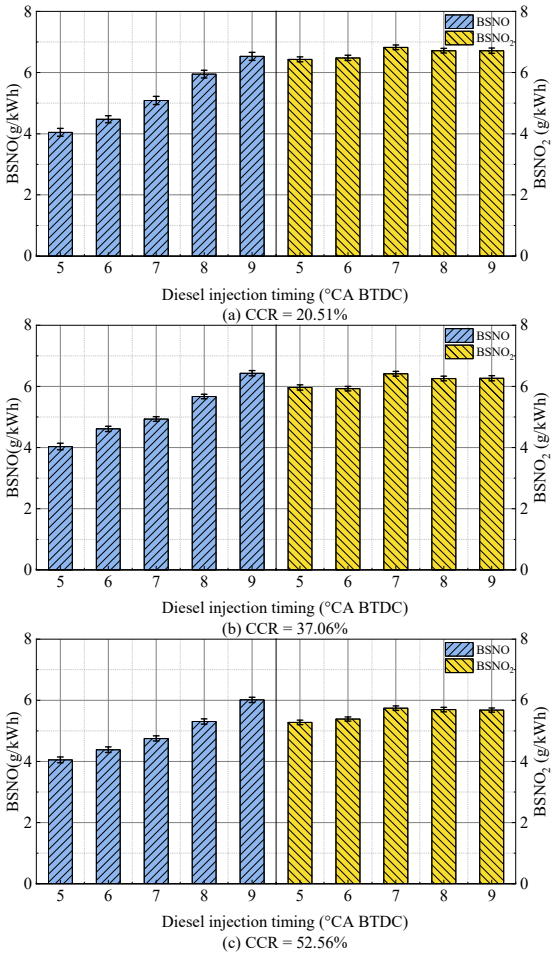

Figure 7. NO and NO_2 emissions with various diesel injection timing.

Moreover, when the DIT is advanced, BSNO will continue to grow under the same CCR, while $BSNO_2$ will increase first and then decrease. The result of BSNO continuous growth may be due to that the advance of DIT will affect the cooling effect of IBE, reduce energy consumption, make the temperature in the cylinder relatively high, and increase the generation of NO. At the same time, due to the advance of diesel injection time, the mixing time of IBE and diesel is shortened. This situation may lead to a fuel-rich area, where more NO emissions will be generated. For $BSNO_2$, when the diesel injection time is later than 7 °CA BTDC, its trend is similar to that of BSNO, and it will gradually increase. NO_2 emissions in exhaust gas are mainly oxidized by NO emissions, and the formation in the cylinder is mainly based on the reaction. The gradually advanced DIT will lead to insufficient combustion of IBE and generate more oxygen-containing groups. At the same time, the increase in NO further promoted the reaction. Therefore, $BSNO_2$ will gradually increase. However, with the further advance of DIT, the premature DIT weakens the cooling effect of IBE and makes the in-cylinder temperature relatively high, which is not conducive to the further conversion of NO. At the same time, premature DIT will affect the distribution of IBE in the cylinder. This leads to a decrease in the area of the main combustion zone and a decrease in the contact area with the unburned part, which also reduces NO_2.

3.3.3. NO_x Emissions

Figure 8 shows the NO_x emissions in the exhaust gas for different DITs. It is obvious that NO_x emissions decrease as the CCR increases when the DIT is the same. However, if the DIT is significantly delayed, the reduction in NO_x emissions decreases slowly. Regarding NO_x emissions, they primarily consist of NO and NO_2. As shown in Figure 7, both NO and NO_2 emissions decrease with an increasing CCR, leading to a reduction in $BSNO_x$. Although NO_2 emissions show some decline for a later DIT, NO emissions remain largely unchanged. Consequently, the decrease in NO_x emissions is limited. When the CCR is the same, NO_x emissions increase as the DIT advances. Meanwhile, when the CCR is high, the growth rate of NO_x emissions slows down. Under the three CCR conditions, $BSNO_x$ increases by 23.9%, 32.7%, and 29.7%, respectively. Initially, when the DIT is advanced, both NO and NO_2 emissions rise, leading to a rapid increase in NO_x emissions. However, as the DIT continues to advance, NO_2 emissions begin to decline while NO emissions still grow. Moreover, the growth rate of NO emissions is faster than that of NO_2 emissions. Consequently, NO_x emissions continue to rise.

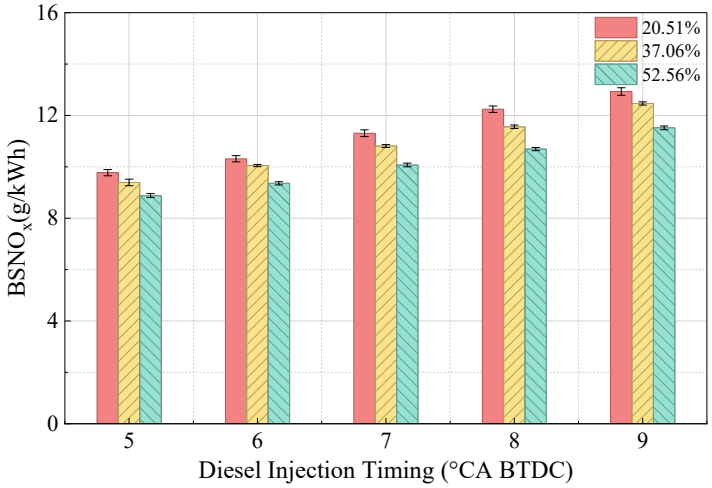

Figure 8. NO_x emissions with various diesel injection timing.

3.3.4. Particle Number Emissions

Figure 9 shows the particle number (PN) emissions in the exhaust gas for different DITs. Under the three CCRs, PN emissions are notably reduced regardless of whether the DIT is advanced or delayed. At the same time, when the CCR is high, PN emissions are significantly reduced. This indicates that when the DIT is fixed, increasing the IBE fraction can effectively reduce PN emissions. Moreover, at a given CCR, adjusting the DIT can also achieve better PN emissions. In addition, under the same test conditions, PN emissions for the original diesel engine ae approximately 7.2×10^5, as shown in Ref. [35]. In terms of soot formation, a higher temperature and lower oxygen content can promote soot formation [39]. When the DIT is delayed, IBE, due to its high latent heat of vaporization, can lower the cylinder temperature, resulting in lower PN emissions. When the DIT advances, the cylinder temperature is higher, which causes a slight increase in PN emissions. But subsequently, due to more complete combustion, the oxygen-containing free radicals formed by IBE combustion increase, which promotes further oxidation of soot particles and reduces PN emissions [40].

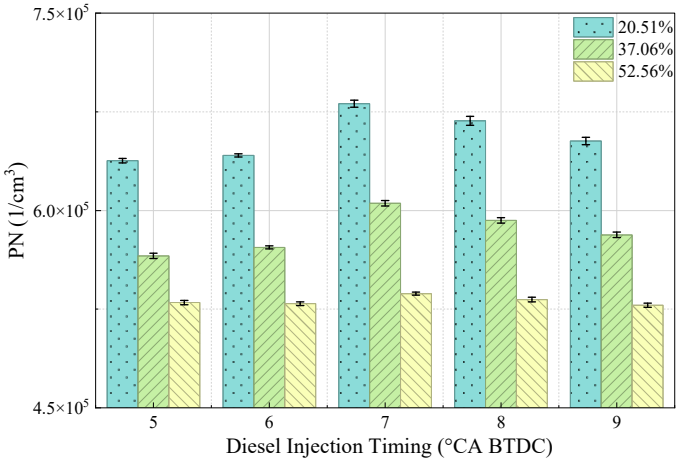

Figure 9. PN emission with various diesel injection timings.

4. Conclusions

This study explores the impact of different DITs on a diesel/IBE dual-fuel engine. Experiments were conducted at CCRs of 20.51%, 37.06%, and 52.56%, with the engine speed at 1600 rpm. The conclusions are as follows:

(1) For the dual-fuel engine used in this study, both the P_{max} and the maximum HRR increase with the advance of DIT. Meanwhile, the corresponding phases are also advanced significantly. As the CCR increases, P_{max} and the maximum HRR both rise as well.

(2) The results indicate that by advancing DIT, the BTE of the dual-fuel engine is improved. Furthermore, the EQBSFC decreases as the DIT advances. This signifies that the engine's fuel economy has been enhanced.

(3) In dual-fuel mode, advancing the DIT can continuously reduce CO emissions. For HC emissions, the minimum occurs when the DIT is 7 °CA BTDC and then increases as the DIT varies. A higher CCR significantly increases both CO emissions and HC emissions.

(4) NO_x emissions increase with the advance of DIT. In addition, PN emissions first increase and then decrease, reaching their peak at 7 °CA BTDC. This result indicates that appropriate delay of DIT can simultaneously reduce NO_x emissions and PN emissions.

Author Contributions: Conceptualization, G.L.; methodology, G.L.; software, Y.Z. and X.L.; validation, K.L.; formal analysis, X.L. and J.W.; writing—original draft preparation, X.L.; writing—review and editing, G.L.; visualization, Y.Z. All authors have read and agreed to the published version of the manuscript.

Funding: This work was supported by the National Natural Science Foundation of China with Grant No. 52306164 and Key Research and Development Projects of Shaanxi Province with Grant No. 2022NY-203. This work was also supported by the Open project of the State Key Laboratory of Engine and Powertrain System (Grant No. Skleps-sq-2025-074). Any findings in this paper are those of the authors and do not necessarily reflect the views of the funding organizations.

Data Availability Statement: The original contributions presented in this study are included in the article. Further inquiries can be directed to the corresponding author.

Conflicts of Interest: The authors declare no conflicts of interest.

Abbreviations

The following abbreviations are used in this manuscript:

ABE	acetone–butanol–ethanol
IBE	isopropanol–butanol–ethanol
CCR	co-combustion ratio
DIT	diesel injection timing
BTE	brake thermal efficiency
BSFC	brake specific fuel consumption
ECU	electronic control unit
PFI	port fuel injection
BTDC	before top dead center
ID	ignition delay
CD	combustion duration
SOC	start of combustion
EOC	end of combustion
HRR	heat release rate
P_{max}	peak in-cylinder pressure
TDC	top dead center
CO	carbon monoxide
HC	hydrocarbon
NO_x	nitrogen oxide
NO	nitric oxide
NO_2	nitrogen dioxide
PN	particle number
SOI	start of injection
HCCI	homogeneous charge compression ignition
RCCI	reactivity controlled compression ignition
PM	particulate matter
CA	crank angle

References

1. Okcu, M.; Varol, Y.; Altun, Ş.; Fırat, M. Effects of isopropanol-butanol-ethanol (IBE) on combustion characteristics of a RCCI engine fueled by biodiesel fuel. *Sustain. Energy Technol. Assess.* **2021**, *47*, 101443. [CrossRef]
2. Sarjovaara, T.; Larmi, M. Dual fuel diesel combustion with an E85 ethanol/gasoline blend. *Fuel* **2015**, *139*, 704–714. [CrossRef]
3. Wang, S.; Zhang, Z.; Hou, X.; Lv, J.; Lan, G.; Yang, G.; Hu, J. The environmental potential of hydrogen addition as complementation for diesel and biodiesel: A comprehensive review and perspectives. *Fuel* **2023**, *342*, 127794. [CrossRef]
4. He, H.; Wang, X.; Wu, J.; Wang, Y.; Fan, F.; Lou, H.; Wang, L.; Liu, K.; Zheng, A.; Liu, L.; et al. Effects of diesel injection timing on performance, regulated and unregulated emissions of a methanol-diesel dual-fuel marine medium-speed engine. *Appl. Therm. Eng.* **2026**, *298*, 130980. [CrossRef]
5. Chen, H.; Su, X.; He, J.; Xie, B. Investigation on combustion and emission characteristics of a common rail diesel engine fueled with diesel/n-pentanol/methanol blends. *Energy* **2019**, *167*, 297–311. [CrossRef]
6. Huang, H.; Lv, D.; Zhu, J.; Zhu, Z.; Chen, Y.; Pan, Y.; Pan, M. Development of a new reduced diesel/natural gas mechanism for dual-fuel engine combustion and emission prediction. *Fuel* **2019**, *236*, 30–42. [CrossRef]
7. Prashant, G.K.; Lata, D.B.; Joshi, P.C. Investigations on the effect of methanol blend on the combustion parameters of dual fuel diesel engine. *Appl. Therm. Eng.* **2016**, *103*, 187–194. [CrossRef]
8. Yang, B.; Ning, L.; Liu, B.; Huang, G.; Cui, Y.; Zeng, K. Comparison study the particulate matter characteristics in a diesel/natural gas dual-fuel engine under different natural gas-air mixing operation conditions. *Fuel* **2021**, *288*, 119721. [CrossRef]
9. Meng, X.; Xie, F.; Li, X.; Wang, X.; Li, X.; Jiang, B.; Liu, Y.; Qian, P.; Zhao, Z. Study on the correlation characteristics of auto-ignition and knocking in high compression ratio spark ignition engine for isopropanol-butanol-ethanol (IBE) blends by dilution strategies. *Energy* **2025**, *340*, 139128. [CrossRef]
10. Han, D.; Fan, Y.; Sun, Z.; Nour, M.; Li, X. Combustion and emissions of isomeric butanol/gasoline surrogates blends on an optical GDI engine. *Fuel* **2020**, *272*, 117690. [CrossRef]

11. Awad, O.I.; Mamat, R.; Ibrahim, T.K.; Hammid, A.T.; Yusri, I.M.; Hamidi, M.A.; Humada, A.M.; Yusop, A.F. Overview of the oxygenated fuels in spark ignition engine: Environmental and performance. *Renew. Sust. Energ. Rev.* **2018**, *91*, 394–408. [CrossRef]
12. Bhumula, K.B.; Kumar, G.N. Effect of fuel injection timing on engine characteristics with an equal volume of 1-heptanol/diesel blend in a CRDI CI engine. *Results Eng.* **2025**, *26*, 104632. [CrossRef]
13. Chockalingam, S.; Ganapathy, S. Performance and Emission Analysis of a Single Cylinder Constant Speed Diesel Engine Fuelled with Diesel-Methanol-Isopropyl Alcohol Blends. In Proceedings of the SAE 2012 International Powertrains, Fuels & Lubricants Meeting, Malmo, Sweden, 18–20 September 2012.
14. Killol, A.; Reddy, N.; Paruvada, S.; Murugan, S. Experimental studies of a diesel engine run on biodiesel n-butanol blends. *Renew. Energy* **2019**, *135*, 687–700. [CrossRef]
15. Atmanli, A.; Yilmaz, N. A comparative analysis of n-butanol/diesel and 1-pentanol/diesel blends in a compression ignition engine. *Fuel* **2018**, *234*, 161–169. [CrossRef]
16. Yu, X.; Wang, T.; Guo, Z.; Zhao, Z.; Li, D.; Li, Y.; Gong, T. Effect of exhaust gas recirculation (EGR) on combustion and emission of butanol/gasoline combined injection engine. *Energy* **2024**, *295*, 130940. [CrossRef]
17. Han, K.; Liu, Y.; Wang, C.; Tian, J.; Song, Z.; Lin, Q.; Meng, K. Experimental study on the evaporation characteristics of biodiesel-ABE blended droplets. *Energy* **2021**, *236*, 121453. [CrossRef]
18. Sun, F.; Chen, H.; Geng, L.; Qi, D.; Wu, H.; Yan, X.; Ji, Z.; Zhang, P.; Chen, Z.; Zhang, W. Study on spray and combustion of acetone-butanol-ethanol (ABE)/biodiesel blends in a constant volume chamber. *Energy* **2025**, *332*, 137180. [CrossRef]
19. Çelebi, Y.; Cengiz, M.; Aydın, H. Propanol and its blend in diesel engines: An extensive review. *J. Energy Inst.* **2025**, *120*, 102047. [CrossRef]
20. Xu, R.; Zhang, Y.; Jiang, X.; Li, F.; Yang, W.; Ma, F. The influence of acetone-butanol-ethanol content on the jet and micro-explosion characteristics during the evaporation of blend fuel droplet. *Fuel* **2025**, *395*, 135224. [CrossRef]
21. Çakmak, A. Comparative research on acetone-butanol-ethanol (ABE) and butanol (Bu) as next-generation biofuels in compression ignition engine. *Therm. Sci. Eng. Prog.* **2024**, *55*, 102956. [CrossRef]
22. Roslan, M.F.; Veza, I.; Said, M.F.M. Effects of injection parameters and intake air temperature on acetone-butanol-ethanol (ABE) blend HCCI-DI engine. *Fuel* **2023**, *345*, 128250. [CrossRef]
23. Zhang, C.; Yang, K.; Li, G.; Dai, J.; Lee, T.H. Spray evaporation characteristics of isopropanol-butanol-ethanol (IBE)/diesel blends in a constant volume chamber. *Fuel* **2022**, *330*, 125659. [CrossRef]
24. Lee, T.H.; Wu, H.; Hansen, A.; Lee, T.; Li, G. Comparison Study on Combustion and Emission Characteristics of ABE/IBE-Diesel Blends in a Common-Rreail Diesel Engine. In Proceedings of the International Powertrains, Fuels & Lubricants Meeting, Beijing, China, 16 October 2017.
25. Meng, X.; Xie, F.; Liu, Y.; Lai, K.; Jiang, X.; Jiang, B.; Zhao, J.; Dou, H. Effect of dilution strategies on the performance and knocking in a spark induced compression ignition (SICI) engine for isopropanol-butanol-ethanol (IBE) blends. *Energy* **2025**, *319*, 134941. [CrossRef]
26. Krishnan, M.G.; Rajkumar, S.; Thangaraja, J.; Devarajan, Y. Exploring the synergistic potential of higher alcohols and biodiesel in blended and dual fuel combustion modes in diesel engines: A comprehensive review. *Sustain. Chem. Pharm.* **2023**, *35*, 101180. [CrossRef]
27. Zeman, J.; Dempsey, A.; Mellesmoen, A.; Omar Duke-Walker, V.; Srna, A. Insights on prechamber enabled mixing-controlled combustion (PC-MCC) with methanol in an optical heavy-duty engine. *Appl. Energy Combust. Sci.* **2026**, *26*, 100479. [CrossRef]
28. Wei, L.; Yao, C.; Wang, Q.; Pan, W.; Han, G. Combustion and emission characteristics of a turbocharged diesel engine using high premixed ratio of methanol and diesel fuel. *Fuel* **2015**, *140*, 156–163. [CrossRef]
29. Tyrewala, D.S.; Kaul, B.C.; Curran, S.J.; Splitter, D.A. Experimental investigation of air-fuel equivalence ratio effects on advanced dual-fuel ammonia/diesel combustion on a single-cylinder medium-duty diesel engine at high load. *Proc. Combust. Inst.* **2025**, *41*, 105794. [CrossRef]
30. Park, S.; Cho, J.; Park, J.; Song, S. Numerical study of the performance and NOx emission of a diesel-methanol dual-fuel engine using multi-objective Pareto optimization. *Energy* **2017**, *124*, 272–283. [CrossRef]
31. Geng, P.; Yao, C.; Wei, L.; Liu, J.; Wang, Q.; Pan, W.; Wang, J. Reduction of PM emissions from a heavy-duty diesel engine with diesel/methanol dual fuel. *Fuel* **2014**, *123*, 1–11. [CrossRef]
32. López, A.F.; Cadrazco, M.; Agudelo, A.F.; Corredor, L.A.; Vélez, J.A.; Agudelo, J.R. Impact of n-butanol and hydrous ethanol fumigation on the performance and pollutant emissions of an automotive diesel engine. *Fuel* **2015**, *153*, 483–491. [CrossRef]
33. Wu, H.-W.; Wang, R.-H.; Ou, D.-J.; Chen, Y.-C.; Chen, T.-Y. Reduction of smoke and nitrogen oxides of a partial HCCI engine using premixed gasoline and ethanol with air. *Appl. Energy* **2011**, *88*, 3882–3890. [CrossRef]
34. Fei, C.; Qian, Z.; Yang, Z.; Ren, J.; Zhu, S.; Yan, Y.; Shu, Z. Combustion and emission performance of isopropanol-butanol-ethanol (IBE) mixed with diesel fuel on marine diesel engine with nano YSZ thermal barrier coating. *Energy* **2022**, *256*, 124683. [CrossRef]
35. Wang, J.; Song, Z.; Li, K.; Li, G.; Che, W. Study on combustion, performance and emission characteristics of a dual-fuel engine fueled with isopropanol-butanol-ethanol (IBE) and pilot diesel. *Appl. Therm. Eng.* **2026**, *297*, 130856. [CrossRef]

36. Li, G.; Lee, T.; Liu, Z.; Lee, C.; Zhang, C. Effects of injection strategies on combustion and emission characteristics of a common-rail diesel engine fueled with isopropanol-butanol-ethanol and diesel blends. *Renew. Energy* **2019**, *130*, 677–686. [CrossRef]
37. Song, E.; Guo, Z.; Guo, L.; Li, S.; Dai, L.; Du, W.; Mu, Z.; Lu, L.; Liu, Z. 1D simulation, performance response analysis, and multi-objective optimization strategy for a marine methanol/diesel dual-fuel engine. *Energy* **2026**, *345*, 140142. [CrossRef]
38. Yaliwal, V.S.; Banapurmath, N.R.; Hosmath, R.S.; Nivedhitha, K.S.; Badruddin, I.A.; Sajjan, A.M.; Ravulapati, K.; Kamangar, S.; Mahamoud, E.R.I. Significance of injection pressure and timing on the combustion characteristics of biodiesel-hydrogen-producer gas-fueled dual fuel and HCCI engines. *Appl. Therm. Eng.* **2025**, *281*, 128675. [CrossRef]
39. Li, G.; Dai, J.; Li, Y.; Lee, T. Optical investigation on combustion and soot formation characteristics of isopropanol-butanol-ethanol (IBE)/diesel blends. *Energy Sci. Eng.* **2021**, *9*, 2311–2320. [CrossRef]
40. Singh, A.; Tsolas, N. Sooting tendency of isopropanol-butanol-ethanol (IBE)/diesel surrogate blends in laminar diffusion flames. *Combust. Flame* **2023**, *250*, 112630. [CrossRef]

Disclaimer/Publisher's Note: The statements, opinions and data contained in all publications are solely those of the individual author(s) and contributor(s) and not of MDPI and/or the editor(s). MDPI and/or the editor(s) disclaim responsibility for any injury to people or property resulting from any ideas, methods, instructions or products referred to in the content.